J Mater Sci (2007) 42:6046–6055
DOI 10.1007/s10853-006-1163-8

Investigation of the ceramifying process of modified silicone–silicate compositions

Jaleh Mansouri · Chris A. Wood · Katherine Roberts · Yi-Bing Cheng · Robert P. Burford

Received: 16 January 2006 / Accepted: 18 October 2006 / Published online: 14 April 2007

Abstract Glass frits were added into silicone-based composites with the aim to improve low temperature ceramification at elevated temperatures. The effect of glass frits on the properties of ceramic residue is investigated. Field emission scanning electron microscopy (FESEM), electron probe microchemical analysis (EPMA) and X-ray diffraction analysis (XRD) showed that glass frits reacted via a eutectic reaction with mica and silica. Electrical conductivity measurements at elevated temperatures showed a decline in volume resistivity with glass frit addition. It was concluded that increased conductivity is a result of ionic conduction of the glass phase produced by eutectic reactions between frits, silica and mica at high temperatures. Thermal mechanical analysis (TMA) was used to explore the dimensional changes of these composites during programmed heat treatment.

J. Mansouri (✉) · R. P. Burford
School of Chemical Sciences and Engineering,
University of New South Wales, Sydney, NSW 2052, Australia
e-mail: j.mansouri@unsw.edu.au

Y.-B. Cheng
Department of Materials Engineering, Monash University,
Clayton, VIC 3800, Australia

C. A. Wood
Air Vehicles Division, Defence Science & Technology
Organisation, Fisherman's Bend, VIC 3207, Australia

J. Mansouri · K. Roberts · Y.-B. Cheng ·
R. P. Burford
Cooperate Research Centre for Polymers, Notting Hill,
VIC 3168, Australia

Introduction

Silicone polymers have been produced commercially since the beginning of the 1940s. Over the past 60 years, silicones have grown into a multimillion-dollar industry with polydimethylsiloxane (PDMS) being the most common member of this class of materials. PDMS-based products include fluids, foams, resins and elastomers and have been used in many fields such as electrical, construction and aerospace industries.

PDMS materials are more fire-resistant than many other organic polymers because both their heat of combustion and heat radiated from the flame to the burning material are substantially lower than those for organic polymers [1–3]. Furthermore, the energies required to depolymerise and volatilise PDMS are significantly larger than those for common organic polymers [4], which means that PDMS combusts and sustains combustion less readily than organic polymers. The deposition of amorphous silica on the surface of PDMS during combustion also provides thermal insulation to the remaining polymer. These attributes make PDMS polymers more suitable for fire resistant applications. As a result, they have been used to improve the fire barrier properties of other polymers. For example, Kashiwagi et al. [5] have shown that when silicone was added to polycarbonate, the rate of heat release during combustion was greatly reduced. Silicone polymers have also been used in the production of ceramics because they can act as a high purity precursor material and are applicable for versatile plastic shaping technologies at low manufacturing temperatures [6, 7].

There have been some attempts to further improve the fire resistance properties of silicone polymers. For example silphenylene-siloxane elastomers were synthesised with a phenyl-silicon-oxygen backbone and pendant vinyl groups.

These polymers have higher decomposition temperature than PDMS (500 vs. 380 °C), indicating that a higher level of heat is needed for their ignition [8–11]. However, these polymers are too expensive for large volume commercial applications.

The powdery silica ash remaining after polymer decomposition is very weak and therefore not suitable for structural applications. It is desirable for polymer compositions used in fire protection applications to maintain their original shape and have sufficient strength.

One approach to improve the strength of the residues is to add inorganic fillers, which could assist densification of the powdery silica through solid-state or liquid phase sintering. From the ceramifying perspective, a high concentration of fillers in the polymer composite would facilitate the formation of a ceramic after polymer decomposition. However, excessive amounts of inorganic fillers could make polymer processing difficult.

Inorganic fillers with a high aspect ratio, such as mica and talc, have been found to provide strength and low shrinkage to residues of polymer-ceramic composites. Weil et al. have found that in thermoplastics, small amounts of high aspect ratio materials such as mica or wollastonite can improve fire-resistance properties of residues by a ''bridging action'' [12], while Marosi et al. proposed the use of polymeric ceramic precursors for forming a protective surface layer [13–15]. They showed that polyboroxo-siloxanes improved the performance and stability of ammonium polyphosphate based intumescent systems, by the formation of silica coated flame retardant particles. In the presence of flame, these particles tend to accumulate on the surface of the polymer and transform to a continuous and protective ceramic-like layer. In spite of much work on the transformation of silicone compositions into ceramics, the mechanism of the transformation and, specifically, the formation of the skin on the surface of ceramic after pyrolysis, have seldom been discussed.

Muscovite mica is a 2:1 layered aluminosilicate that has been of particular interest for electric insulation because of its outstanding corona resistance and insulation properties [16]. Our previous work has shown that a degree of strength was achieved in pyrolysed silicone–mica compounds when muscovite mica was combined with silica residue. This was shown to result from localised liquid formation at silica/mica interfaces via a eutectic reaction [17, 18]. Whilst effective at high temperatures (around 1,000 °C), strength development at lower temperatures remained poor. A ceramifying compound, when exposed to increasing degrees of heat, would ideally transform from a polymeric material into a strong, hard ceramic material with no weak, intermediate stage. In practice this may be difficult to achieve as silicone decomposes to a soft, powdery silica at approximately 350–500 °C, whilst the liquid phase formed from eutectic reactions between mica and silica does not occur until much higher temperatures (above 800 °C). Thus there is a need to improve low temperature strength and also increase high temperature strength.

The approach taken in the current work is to use glass additives (glass frits) to improve the low temperature strength of silicone/mica compositions. Two types of glass frits with low softening points, and another with a high softening point, were examined for their ability to improve the strength of pyrolysed silicone/mica compositions at both intermediate and high temperatures. Samples from each of these compositions were heated to different temperatures and their strength and dimensional changes were estimated. FESEM, EPMA, TMA and XRD were used to study the ceramifying process. Residue electrical conductivity issues were also addressed, by evaluating the changes in volume resistivity of compositions with respect to temperature.

Experimental

Materials

All materials were used as received.

Elastosil® R401/80S, a silicone gum from Wacker-Chemie GmbH (Table 1), was used in this work.

Dicumyl peroxide (Di-Cup 40C, cure temperature range: 160–170 °C; Akzo-Nobel) in powder form was used as the curing agent.

Two different muscovite micas with different particle sizes were used. Mica MT60C (Mica A) is coarse muscovite mica manufactured by MinTech International, Bloomington, IN, USA. Greater than 90% is retained on a 100 mesh (150 μm) screen, and 99% is retained on a 240 mesh (63 μm) screen. XRF analysis showed a composition of SiO_2: 55.15%; Al_2O_3: 29.98%, Fe_2O_3: 1.95%, MgO: 0.72%, CaO: 0.03%, SO_3: 0.24%, MnO: 0.05%; Na_2O, 0.77%; K_2O, 8.33%; TiO_2, 0.13%; P_2O_5, 0.03%, minor oxides and volatile compounds: 2.62%.

Mica F260 (Mica B) is dry-ground fine muscovite mica manufactured by Oglebay Norton Specialty Minerals,

Table 1 Properties of Elastosil® 401/80S silicone rubber

Density, g/cm^3[a]	1.17
Hardness, Shore A unit[a]	75–85
Glass transition, °C[b]	–122
Cold crystallisation, °C[b]	–80
Melting point, °C[b]	–39

[a] From suppliers catalogues

[b] Measured by differential scanning microscopy (DSC)

Kings Mountain, NC, USA and supplied by Omya Southern Pty. Ltd. About 34% is retained on a 400 mesh (38 μm) screen and 8.5% retained on a 200 mesh (75 μm) screen. It had a composition of SiO_2: 49.88%; Al_2O_3: 31.90%, Fe_2O_3: 2.58%, MnO: 0.08%, CaO: 0.02%, SO_3: 0.25%, Na_2O, 0.76%; K_2O, 8.87%; TiO_2, 0.24%; P_2O_5, 0.05% and other minor oxides and volatile components: 5.37%. Muscovite mica was chosen as it is expected that its alkali component would promote the formation of a liquid phase during heating at elevated temperatures.

Frits are ground glass of a desired particle size distribution supplied by Ferro Corporation (Australia) Pty. Ltd. One of the main factors considered in selecting glass additives for these compositions was the glass softening point. This is because it indicates the temperature at which the viscosity of the glass additive decreases enough for glass to flow and begin to bind pyrolysis products and other inorganic components together. The softening point of a glass is defined as the temperature at which it has a viscosity of $10^{6.6}$ dPa s [19].

Softening points and chemical compositions of glass additives were estimated by the method described in Sect. ''Softening point of glass frits'' and XRF, respectively, and summarised in Table 2. The Loss on Ignition values (LOI, an approximate measure of volatile components) were 7.7, 14.4 and 8.7 wt% for glass frits C, D and E, respectively.

Sample preparation

All compounds were prepared using a conventional two-roll mill, with silicone rubber first softened at room temperature and fillers then added until a homogeneous batch was obtained. The curing agent was then added and processed until a visually good dispersion was achieved. Silicone compounds were moulded and cured into flat sheets by compression moulding at 175 °C for 20 min under 7 MPa pressure.

Sample pyrolysis

Pyrolysis of flat sheet samples (50 × 14 × 2 mm) was performed using a muffle furnace. Samples were heated from room temperature to target temperatures using a heating rate of 12 °C/min.

Characterisation

X-ray fluorescence (XRF)

Chemical compositions of mica and glass frits were analysed by the X-ray fluorescence method using a Philips PW2400 XRF spectrometer. Glass sample disks (40 mm diameter) were prepared using a mixture of flux (borate glass and ammonium nitrate) and sample in an approximate ratio of 5.43:1. The mixture was heated in a platinum-gold crucible for 15 min at 1,050 °C by which time the sample had dissolved. The melt was poured into a graphite disc held on a hot plate at about 220 °C. An aluminium plunger was then brought down to gently mould and quench the melt [20].

Morphological studies

Field emission scanning electron microscopy (FESEM) observations of both cured and ceramified silicone compounds were made using a Hitachi S4500II instrument. Samples were sputter-coated with either gold or carbon using a Polaron Sputter coater unit.

Microchemical mapping analysis

A Cameca SX-50 microprobe was used to carry out the microchemical mapping of the residue ceramics. Calibration was carried out using certified standard reference materials for silicon, potassium and aluminium. The concentration of each element present in the area of interest was determined in two dimensions. Typically the analysed area was divided by 256 × 256 pixels with 0.2 μm/pixel and the intensity was measured at each pixel. For these measurements samples were embedded in epoxy resin, polished and made conductive by carbon coating.

Flexural strength measurements

The flexural strength of pyrolysed samples was determined by the 3-point bend method using an Instron Universal Testing Machine. Samples measuring 50 × 14 × 3 mm were heated at various temperatures and held at the target temperature for 30 min. Loads were applied at a rate of

Table 2 Chemical compositions (wt.%) and softening point (°C) of glass frits

Ferro code	Code for this work	Softening point, (°C)	Chemical composition, wt%									
			SiO_2	Al_2O_3	CaO	Na_2O	K_2O	ZnO	TiO_2	P_2O_5	V_2O_5	Fe_2O_3
EAP8017	C	525	33.5			18.2	10.8		19.3	1.8	8.7	
EAP8053	D	525	37.7	1.2	1.2	14.6	10.6		16	1.3		3.0
KMP4103	E	800	39.2	5.5	5.3	2.9	2.2	36.2				

0.5 mm/min. Flexural strength was calculated using Eq. (1):

$$S = \frac{3PL}{2bd^2} \quad (1)$$

where P is the maximum load (N), L is the outer support span (mm), b is the specimen width (mm) and d is the specimen thickness (mm), to give S in MPa.

Thermal characterisation

(a) Thermal transitions of silicone elastomer compounds

Glass transitions, crystallisation and melting points of raw rubbers were determined using a 2010 Differential Scanning Calorimeter (TA Instruments). Samples were cooled from room temperature to –160 °C and then heated to 250 °C at 20 °C/min in a nitrogen environment.

(b) Thermomechanical analysis (TMA)

TMA expansion mode was used. A quartz cylindrical expansion probe rested on the surface of the test specimen with a 0.02 N load applied. Displacement was measured as the temperature was raised from 20 to 950 °C, using a TA Instruments TMA 2940 unit.

X-ray diffraction analysis (XRD)

Wide angle X-ray scattering was conducted using a Philips PW1830 generator with a 371 mpd control. The scan was conducted from a 2θ angle of 2° to 60° at a scan rate of 1°/min.

High temperature electrical resistivity measurements

A procedure was developed to measure the electrical resistivity of the ceramic materials at high temperatures, which uses a 40 mm square sheet of the polymeric compound. This sits on a copper sheet electrode that is larger than the sample. An upper square electrode (25 × 25 mm) is then centred on top of the sample. Rigid electrically insulating weights sit on top of this stack to keep components in place. Thin 1.5 mm^2 cables insulated with non-burning insulation are attached to each of the electrodes. The whole unit is then placed inside a muffle furnace. The two wires leading to each of the electrodes are able to protrude from the closed furnace door. Soft kaowool insulation is used to add extra electrical insulation to the electrode wires. The muffle furnace can then be heated and the electrical resistance across the sample can be measured. Measurements were made on samples at temperatures up to 1,000 °C.

A DC power supply was used to measure both voltage and current with a known voltage across the sample. The current is measured and the resistance, R, is then calculated using Ohm's Law. With known thickness, t, and area of the sample prior to the test, A, the volume resistivity, ρ_v, can be calculated using Eq. (2):

$$\rho v = \frac{R \times A}{t} \text{ (ohm - cm)} \quad (2)$$

where R, A and t are in units of ohms, cm^2 and cm, respectively. Volume resistivity is a more useful value than resistance, as it is an intrinsic material parameter, and therefore allows direct comparison between different compositions.

Shrinkage properties

Shrinkage of a range of compositions was measured by heating flat sheet samples sandwiched between thin stainless steel plates to 600, 800 and 1,000 °C for 30 min in air. To avoid any bloating effects, the length and width changes of the sample were measured and the average calculated, correcting for any changes in the thickness of the samples that may have arisen from bloating.

Softening point of glass frits

A technique to estimate the softening point involves forming a solid body with sharp edges from the glass frit and heating it to various temperatures. The temperature at which the sharp edges of the glass begin to change can be considered the softening point. Whilst lacking absolute accuracy, it was found to be satisfactory for the comparison of different glasses. Fourteen millimeter diameter cylindrical pellets of the glass additives were compressed and heated in steps of 25 °C. The furnace was held at each temperature for 30 min to allow time for the glass to begin to flow at each temperature. The temperature at which the edges of the pellet began to round off or at which the pellet began to slump is considered to be the softening point of the glass.

Results and discussion

Dimensional changes of ceramifying compositions fired at different temperatures

Dimensional changes of ceramified samples were measured and show that addition of fine mica B and glass frits to a silicone/mica A base composition increased the shrinkage at 1,000 °C, but decreased expansion at lower temperatures (Table 3). Shrinkage at 1,000 °C increased when low temperature glass frits (C and D) are added, compared with the high temperature glass frit E. Increasing the level of liquid phase at high temperatures by adding glass frits increased the 1,000 °C shrinkage that occurred at 1,000 °C. This is expected if liquid phase sintering is via the

Table 3 Dimensional changes of different silicone compositions at different temperatures

Compositions	Shrinkage (–)/expansion (+) (%)		
	600 °C	800 °C	1,000 °C
Silicone/mica A/peroxide (78:20:2)	1.5	0.57	–0.73
Silicone/mica A/peroxide/glass frit E (75.5:20:2:2.5) (composition H)	0.64	0.59	–3.5
Silicone/mica A/peroxide/glass frit D (76.75:20:2:1.25)	–0.37	–1.2	–5.7
Silicone/mica A/peroxide/glass frit D (75.5:20:2:2.5)	–0.8	–1.96	–5.4
Silicone/mica A/peroxide/glass frit D/glass frit E (75.5:20:2:1.25:1.25)	0.26	–0.17	–5.9
Silicone/mica A/mica B/peroxide (68:20:10:2) (composition F)	1.10	0.3	–1.3
Silicone/mica A/mica B/peroxide/glass frit C (65.5:20:10:2:2.5) (composition G)	0.92	0.2	–6.3

Note: Numbers in brackets are weight percent of each component in the composition

densification mechanism, as a greater volume of liquid phase would allow for more rapid particle rearrangement.

Compositions made with glass frits C and D showed limited shrinkage at 600 and 800 °C, which contrasts with other compositions, which expand at these temperatures. This indicates that a degree of sintering may have occurred in these compositions, which could result in a stronger material. When high softening point glass frit E was added to the base composition, no significant dimensional changes occurred up to 800 °C. In contrast to the results for the lower temperature, heating at 1,000 °C caused significant shrinkage, due to the formation of a liquid phase, that allows densification via liquid phase sintering. This mechanism was not observed at lower temperatures, because insignificant amounts of low viscosity liquid phase are produced.

Mechanical strength

The flexural strengths of different compositions pyrolysed at various temperatures are summarised in Table 4.

For samples heated at 800 °C, addition of low softening point glass frits (C and D) leads to a significant increase in the flexural strength of the residue samples. When half of glass frit E is replaced with glass frit D, the flexural strength of the ceramified residue improved, at all heating temperatures. When heated at 1,000 °C, the combinations of silicone/mica/glass frit produced flexural strengths of 1.88 MPa with 2.5% glass frit E. With 1.25 wt.% of glass frits D and E the flexural strength increased to 4.84 MPa. Strength at 600 and 800 °C was increased by low temperature glass frits 5-fold. The addition of the high softening point glass frit (frit E) had an insignificant effect on strength for samples heated at 600 °C when compared with no glass frit. Similarly, little effect is seen at 800 °C for frit E. However, the low softening point frit increases strength compared with the equivalent compositions with no glass frit or with high softening point glass frit. Glass frit E becomes active only at 1,000 °C, and then provides significant improvements in flexural strength.

Microstructural studies

To investigate the mechanism of ceramic formation, compositions F and G (Tables 3, 4) were selected for

Table 4 Flexural strength of different silicone compositions at different temperatures

Compositions	Flexural strength (MPa)		
	600 °C	800 °C	1,000 °C
Silicone/mica A/peroxide (78:20:2)	[a]	0.34	0.64
Silicone/mica A/peroxide/glass frit E (76.75:20:2:1.25)	0.12	0.34	1.70
Silicone/mica A/peroxide/glass frit E (75.5:20:2:2.5) (composition H)	0.1	0.32	1.88
Silicone/mica A/peroxide/glass frit D (76.75:20:2:1.25)	0.64	1.65	2.92
Silicone/mica A/peroxide/glass frit D (75.5:20:2:2.5)	0.88	2.30	3.53
Silicone/mica A/peroxide/glass frit D/glass frit E (75.5:20:2:1.25:1.25)	0.52	1.9	4.84
Silicone/mica A/peroxide/glass frit C (76.5:20:2:2.5)	0.68	2.14	3.21
Silicone/mica A/mica B/peroxide (68:20:10:2) (composition F)	0.12	0.42	0.93
Silicone/mica A/mica B/peroxide/glass frit C (65.5:20:10:2:2.5) (composition G)	0.65	2.54	3.89

[a] Too weak to be measured

Note: Numbers in brackets are weight percent of each component in the composition

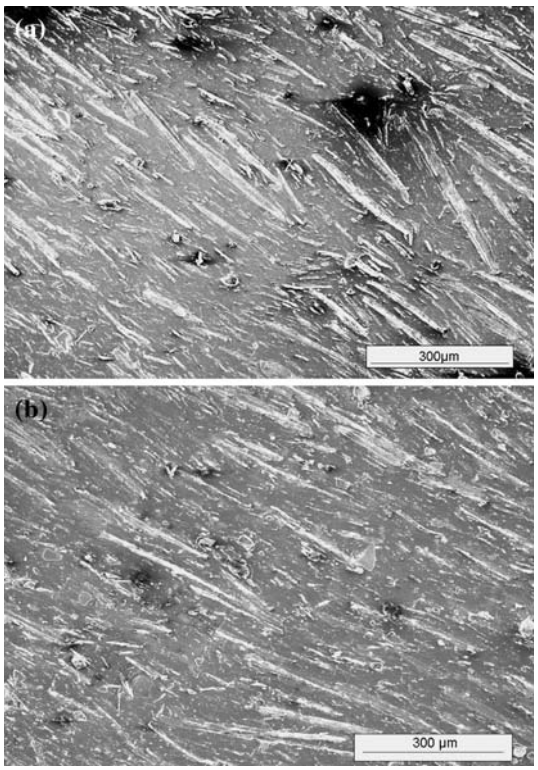

Fig. 1 Microstructure of cross-section of samples at room temperature (**a**) composition F and (**b**) composition G

microstructural and microchemical analysis using FESEM and EPMA techniques. It was expected that a mixture of micas (with different particle sizes) and the presence of vanadium in the glass frit C should contribute to glass forming at low to medium temperatures. Ceramifying samples were prepared by heating the compositions in a muffle furnace in air for 30 min at 1,000 °C.

Samples were embedded in epoxy resin, sliced crosswise and polished to give a flat and smooth surface. Prior to heating, both compositions had a similar morphology, with fillers uniformly dispersed in the silicone rubber matrix. The highly oriented nature of mica particles in the matrix after compaction is also evident (Fig. 1).

Figures 2 and 3 show SEM images at high temperatures. The fracture surface of composition F shows localised melting of mica particles at the edges and bridging between mica plates and pyrolysis products after heating to 1,000 °C (Fig. 2a). When glass frits were used, the matrix became glassy and porous, Fig. 2b, indicating that the glass frit had facilitated bonding between the mica particles and the silica originated from pyrolysis of silicone. The bonding between mica and matrix in composition G is more advanced and the particle size of the matrix was noticeably increased by addition of glass frit. The higher strength of composition G than composition F (Table 3) can be attributed to these differences in microstructure.

Smooth polished cross-sections of samples heated to 1,000 °C are shown in Fig. 3. For composition F the mica plates are mostly isolated and in one case, the de-bonding between mica and matrix is evident, which indicates rather poor adhesion of mica to the matrix. In contrast, mica particles in composition G show advanced local melting and in many cases they are inter-connected through micro-bridges of the liquid phase. However, this eutectic liquid phase can be conductive (Sect. ‘‘Electrical resistivity at

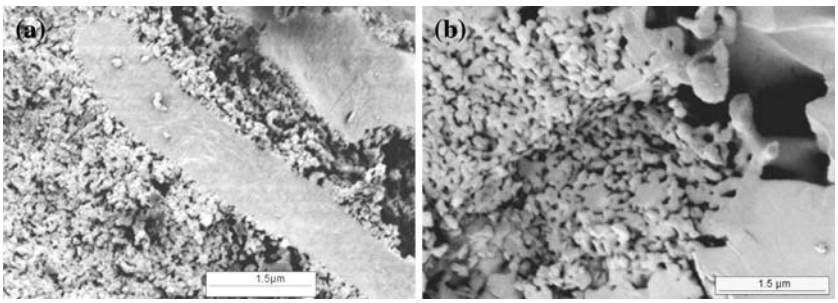

Fig. 2 Fracture surface of (**a**) composition F and (**b**) composition G after heating to 1,000 °C for 30 min

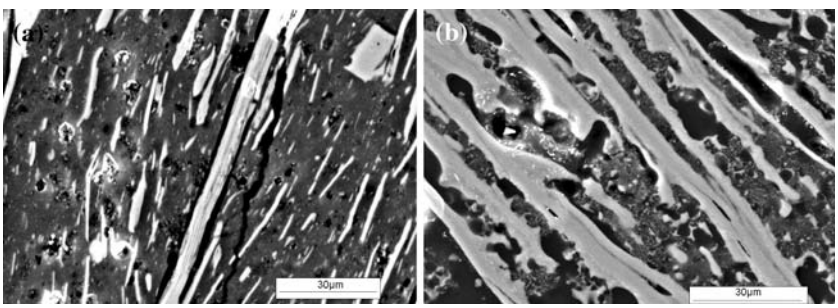

Fig. 3 FESEM of polished sections of (**a**) composition F and (**b**) composition G

elevated temperatures''). Thus may provide a continuous conducting path leading to lower resistivity at high temperatures, limiting the use of these compositions in certain applications including cable insulation. For example, in emergency power supply circuits, there is a requirement for electric cables to continue to operate and provide circuit integrity, even when subjected to fire (and water spray). Thus it is important that the insulation maintains a sufficiently high electrical resistivity even after prolonged heating at elevated temperatures.

Localised micro-chemical analysis

Cross-sections of samples fired at 1,000 °C were studied by EPMA in mapping mode. For composition F (images are not shown here) these results showed very low amount of glass (mainly rich in silica) at the edges of the mica. Trace amounts of potassium and sodium may diffuse from mica to the adjacent areas in the matrix, but they could not be detected by microprobe analysis.

An overview of the cross-section of composition G (prepared with the same method which was described in Sect. ''Microstructural studies'') is shown in Fig. 4 and shows consistent liquid formation. The mapping area and signals for different elements in a 50 μm square area are given in Fig. 5 and show that both Na and K are present in mica and the matrix. Potassium and sodium alkali have diffused into the matrix, assisting glass formation via a eutectic reaction. Vanadium is present at the edges of the mica particles and to a lesser extent in the glassy region. As only original component that contains vanadium is the glass frit, this indicates that vanadium was mobilised by heating and has contributed to the eutectic reaction. Microbridges between mica particles can be seen in Fig. 5c. They contain mainly silicon with some vanadium and potassium (Fig. 5b, e), confirming the contribution of these elements to the glass formation.

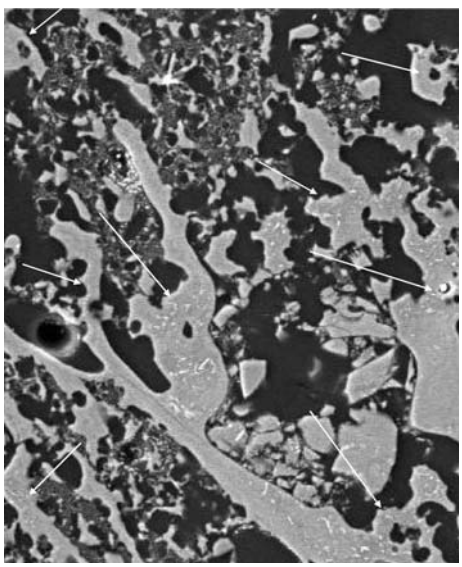

Fig. 4 An overview of the cross-section of composition G. Liquid regions are shown by arrows

XRD analysis

XRD spectra for the mixture of mica A and mica B before and after heat treatment and for composition F and composition G after heating to 1,000 °C for 30 min are given in Figs. 6 and 7. These patterns show that.

- The XRD pattern for the mica mixture possesses all peaks of the 2M1 type muscovite [21] together with some impurities such as quartz and kaolin.
- More liquid phase was formed at 1,000 °C, as shown by the appearance of a large hump around $2\theta = 24°$ confirming the presence of an amorphous phase in the product.
- Mica in composition F remained approximately the same before and after heat treatment at 1,000 °C, but disappeared in composition G after heating and cristobalite became a major phase. This suggests that the addition of low temperature glass frit facilitates the decomposition of mica, leading to an increased amount of liquid phase for solidification.

Dimensional change and thermal expansion coefficient

Figure 8 shows the TMA trace for composition F. The first linear part (20–360 °C) is a constant slope of dimensional change before polymer pyrolysis, representing a thermal expansion coefficient about of 440×10^{-6} m/m °C. Above 360 °C, there is a rapid increase in expansion (from 17% to 62%) due to the evolution of gases during pyrolysis. Optical images taken after the TMA test showed bloating and crack for Composition F (see Fig. 10). Shrinkage was recorded between 550 and 1,000 °C due to liquid phase assisted densification, showing an average thermal shrinkage of 120×10^{-6} m/m °C, which was a result of sintering.

Composition G had a similar thermal expansion coefficient (about 424×10^{-6} m/m °C) to F below 350 °C (Fig. 9). However a much lower expansion (11%) compared to composition F was seen at above 350 °C, probably due to the expansion derived from polymer pyrolysis being compensated by the shrinkage due to sintering. The sample showed no large cracks after the TMA test (Fig. 10b). At temperatures above 430 °C, consecutive dimensional changes with thermal expansion coefficients of –118 (430–625 °C), –138 (625–770 °C), –387 (765–835 °C) and -143×10^{-6} m/m °C (835–950 °C) occur. These differences in sintering rates may indicate different stages of

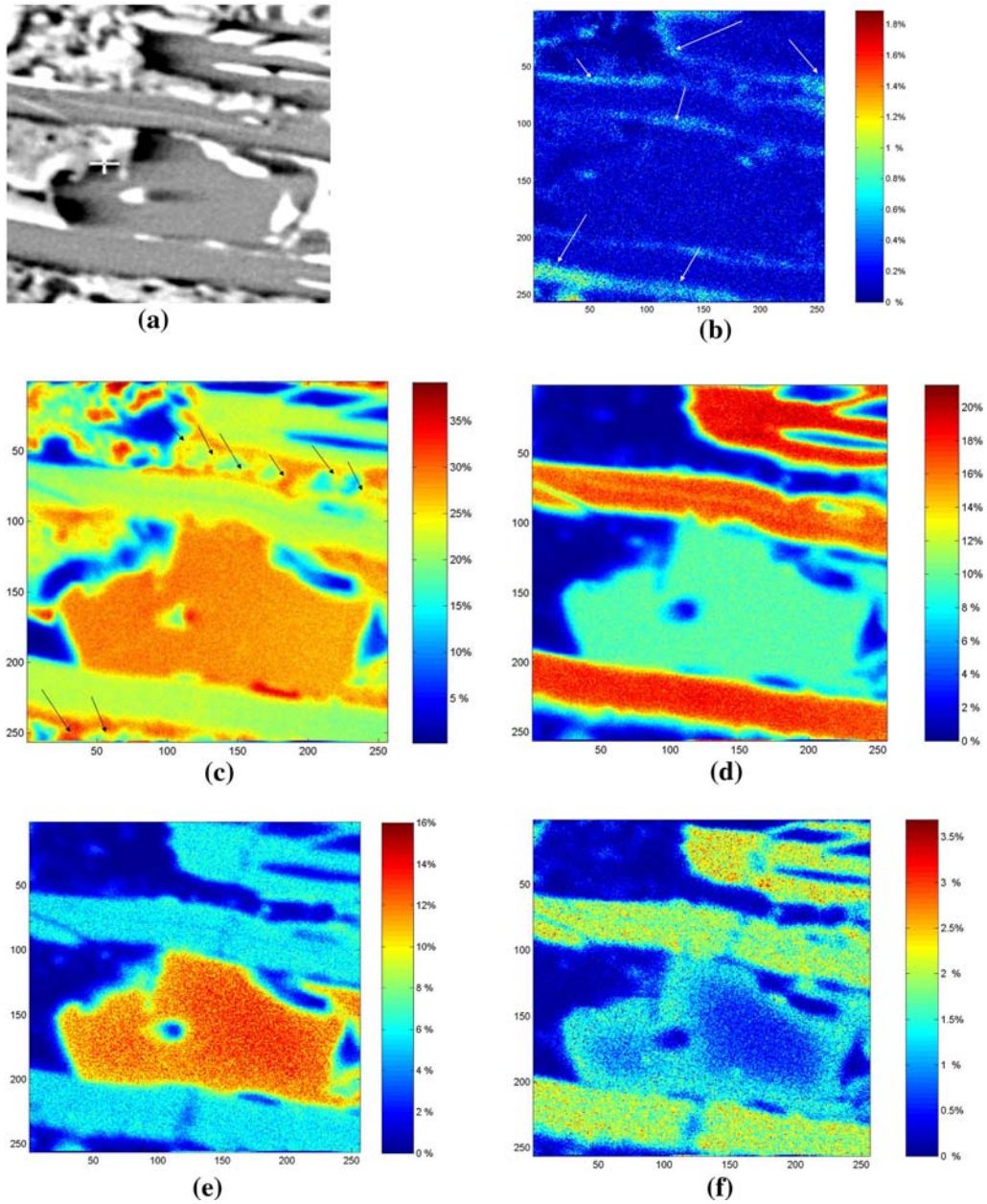

Fig. 5 About 50 μm square area of composition G heated at 1,000 °C, (**a**) backscattered image, (**b**) vanadium, (**c**) silicon, (**d**) aluminium, (**e**) potassium and (**f**) sodium signals. Arrows in (**b**) show areas rich in V and in (**c**) show the micro bridges

reactions leading to the formation of the liquid phase in this multi-component system.

Electrical resistivity at elevated temperatures

Whilst the use of glass frit additives improves strength, it is critical to evaluate the electrical conductivity of the pyrolysed compounds at elevated temperature if the material is to be suitable for fire-resistant cable applications. The test described in Section ''High temperature electrical resistivity measurements'' measures the volume resistivity of the compositions at high temperatures using flat sheet samples. The results of the measurement are plotted in Fig. 11 for the following compositions (see Table 3 for compositions F, G and H). Composition S is silicone rubber with 2 wt.% peroxide.

These results show a steady decrease in resistivity with increasing temperature for all compositions. Silicone polymer containing no additional fillers (composition S) exhibits a relatively high volume resistivity, up to 1,000 °C. The addition of 30% muscovite mica (composition F) dramatically reduces the volume resistivity of the

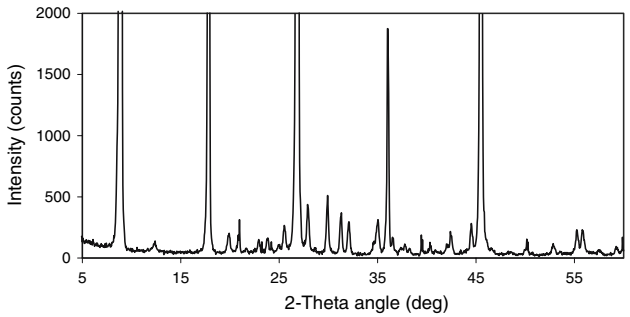

Fig. 6 XRD spectrum for the mixture of mica A and mica B at room temperature

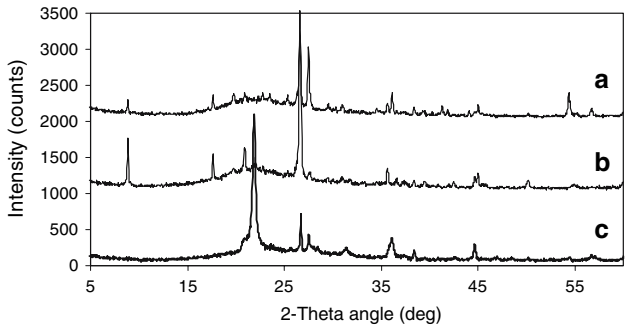

Fig. 7 XRD spectra of (**a**) mixture of mica A and mica B (**b**) composition F and (**c**) composition G after heating to 1,000 °C for 30 min

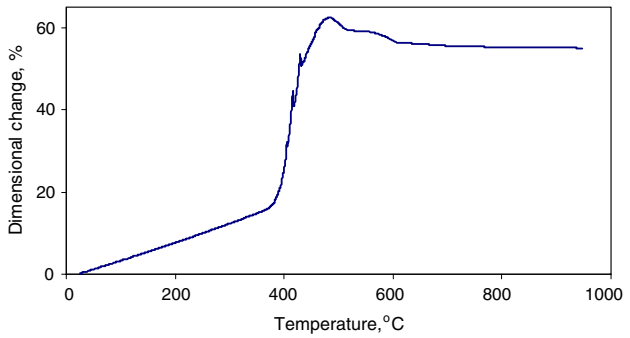

Fig. 8 TMA trace for composition F between room temperature and 950 °C at a heating rate of 10 °C/min in static air

silicone material, by an order of magnitude at 1,000 °C. It is thought that this increased conductivity results from ionic conduction in the glass phase that is created by eutectic reactions between silica and mica on heating.

Conductivity of glasses depends on glass composition. Alkali ions such as Li^+, Na^+, and K^+ are relatively small and thus quite mobile in the glass network [22, 23]. These alkalis, especially Na^+, are very common in a wide range of glasses as they are effective network modifiers, used to lower the melting temperature of glasses. Muscovite mica

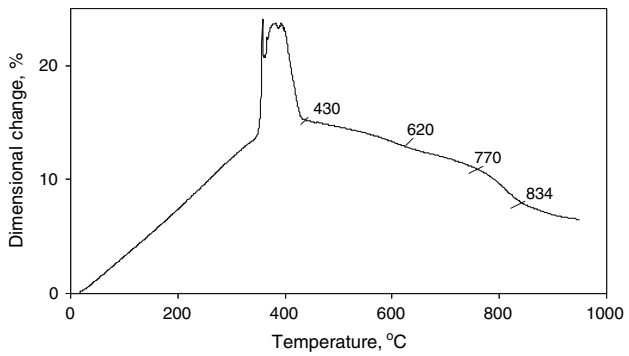

Fig. 9 TMA trace of composition G between room temperature and 950 °C at a heating rate of 10 °C/min in static air

has a nominal composition of $KAl_3Si_3O_{10}(OH)_2$ and also contains sodium as a major impurity. When muscovite and silica react via a eutectic reaction at high temperature, they form a liquid phase that contains potassium and sodium. The relatively mobile K^+ and Na^+ ions then increase electrical conductivity at elevated temperature.

Further evidence of the role of glass in electrical conductivity can be seen when glass frits were added to the silicone-mica compositions. The addition of 2.5% glass frit C (composition G) led to significant reduction in volume resistivity, being two orders of magnitude lower than that for the silicon/mica compound (composition F), and three orders lower than for the silicone only material (composition S).

XRF results show that glass frit C contains 18.2 wt.% Na_2O and 10.8 wt% K_2O. Given this very high alkali content, high conductivity of the material containing the frit is expected at elevated temperature. This glass frit also contains vanadium, which is a transition metal. It is reported that the presence of transition metal ions can make oxide glasses conductive [24]. On the other hand, glass frit E contains only 2.9 wt.% Na_2O and 2.2 wt.% K_2O. The replacement of glass frit C by glass frit E (composition H), provides higher volume resistivity.

In summary, the addition of any alkali-containing filler to silicone, whether it is muscovite mica or a glass frit, has the potential to increase conductivity of silicone based composites at high temperatures if conductive ions can be liberated via melting or dissolution. It is also clear that alkali-containing glasses increase conductivity more than mica. When mica particles react with the silica matrix at the fire testing temperature (1,000 °C), melting takes place only at mica particle edges, with most of alkali ions being still bound in the crystalline structure of mica. Because this would only release a limited amount of alkali ions to the liquid phase, the increase in material conductivity is less. Glass does not have a fixed melting point and softens with increasing temperature. Above the glass softening point, all

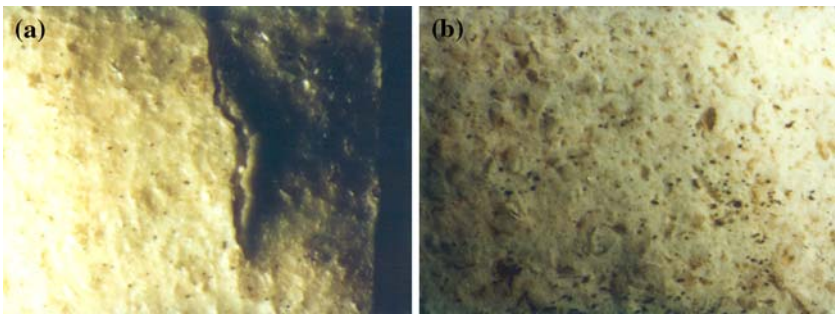

Fig. 10 Optical microscopy images of top surface of (**a**) composition F and (**b**) composition G after TMA analysis (mag: (16)

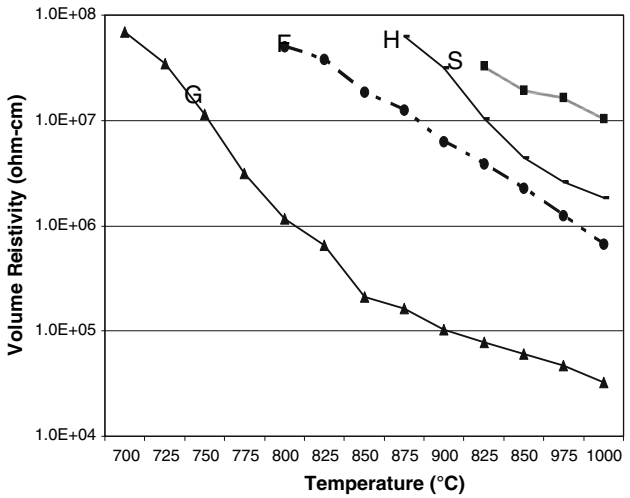

Fig. 11 Volume resistivity versus temperature for different silicone compositions

alkali ions in a glass become mobile and contribute to ionic conduction under an electric field.

Conclusion

The requirement for low temperature ceramification means that it would be insufficient to rely on purely the mica-silica eutectic reaction, which takes place above 800 °C. The addition of glass frits is a useful technique for lowering the temperatures at which strength is developed in pyrolysed compositions. These glass frits melt at temperatures below the mica-silica eutectic temperature and combine with the inorganic fillers and pyrolysis products of silicone rubber to assist the formation of a ceramic. FESEM, XRD and EPMA analyses showed that glass frits react with fillers and the silica matrix to form a liquid phase which bonds the fillers and silica matrix together, rendering strength to the char. However, compositions with glass frits became conductive at high temperatures. It was found that for an equivalent reduction in resistivity, much higher loadings of mica can be used, compared to glass frits.

Acknowledgements The authors thank Dr E. Slansky for his help with the XRD analysis, Ms Irene Wainwright for her help with the XRF analysis and Mr B. Searle for his help with the EPMA.

References

1. Lipowitz J (1982) J Fire Flammability 15:39
2. Hshieh FY (1998) Fire Mater 22:69
3. Buch RR (1991) Fire Saf J 17:1
4. Lipowitz J (1976) Fire Flammability 7:482
5. Kashiwagi T, Clearly G, Davis GC, Lupinski JH (1993) A non-halogenated, flame retarded polycarbonate. In: Proceedings of the international conference for the promotion of advanced fire resistant aircraft interior materials. Federal Aviation Administration Technical Center, Atlantic City, New Jersey, p 157
6. Baldus HP, Wagner O, Jamsen M (1992) Mater Res Soc Symp Proc 271:821
7. Riedel R, Passing G, Schonfelder H, Brook RJ (1992) Nature 355:714
8. Dvornic PR, Lenz RW (1990) High temperature siloxane elastomers. Huethig & Wepf Verlag, New York
9. Dennis H, Zhu HD, Kantor SW, Macknight WJ (1998) In: Lyon RE (ed) Fire resistant materials: progress report, Final Report DOT/FAA/AR-97/100. U.S. Department of Transportation, Washington, DC, November 1998, p 59
10. Lauter U, Kantor SW, Schmidt-Rohr K, Macknight WJ (1999) Macromolecules 32:3426
11. Zhu HD, Kantor SW Macknight WJ (1998) Macromolecules 31:850
12. Weil ED (1987) Plastics compounding (January–February) 31:40
13. Marosi G, Marton A, Anna P, Bertalan G (2002) Polym Degrad Stab 77:259
14. Marosi G, Csontos I, Ravadits I, Anna P, Bertalanand G, Toth A (1999) Recent Adv Flame Retard Polym Mater 10:88
15. Marosi G, Ravadits I, Bertalan G, Anna P, Maatoug MA (1998) In: Fire retardancy of polymers: the use of intumescence. The Royal Chemical Society, Cambridge, p 325
16. Hepburn DM, Kemp IJ, Shields AJ (2000) IEEE Elect Insul Mag 16(5):18
17. Mansouri J, Burford RP, Cheng YB, Hanu L (2005) J Mater Sci 40:5741
18. Mansouri J, Burford RP, Cheng Y-B (2006) Mater Sci Eng A 425:7
19. Norrish K, Hutton JT (1969) Geochim Cosmochim 33:431
20. Barlow G, Manning DA (1998) Br Ceram Soc Trans 97:122
21. Fujino S, Ijiri H, Shimizu F, Morinaga K (1998) J Jpn Inst Metals 62(1):106
22. Meunier M, Currie JF, Wertheimer MR, Yelon A (1983) J Appl Phys 54(2):898
23. Ngai KL (1996) J Non-Cryst Solids 203(1):232
24. Ungureanu MC, Levy M, Souquet JL (2000) Ceramics—Silikaty 44(3):81